

# Avalanche Photodiode with High Dynamic Range, High Speed and Low Noise

Alberto Ciarrocchi <sup>(1)</sup>, Wei Quan <sup>(1)</sup>, Maria Hämmerli <sup>(1)</sup>, Hektor Meier <sup>(1)</sup>

<sup>(1)</sup> Albis Optoelectronics AG, Moosstrasse 2A, 8803 Rueschlikon, Switzerland, [hm@albisopto.com](mailto:hm@albisopto.com)

## Abstract:

*This paper reviews recent advances and novel applications of state-of-the-art III-V avalanche photodiodes. We demonstrate a record sensitivity of -34.5 dBm and -27 dBm, for 10 Gb/s and 25 Gb/s APDs respectively, with a high optical damage threshold above +6 dBm. ©2022 The Author(s)*

## Introduction

High speed, avalanche photodiodes (APD) are used in various applications reaching from telecom and datacom, to free-space and sensing. The main advantage of an APD receiver versus a photodiode (PD) based solution is its improved sensitivity. High sensitivity, high speed APD receivers are important for extended reach optical interconnects in telecom and datacom where the tight link budget requires additional receiver sensitivities. With higher bit rate in data communication and more complex data formats, the demand for fast APDs is growing.

Under the strong electric fields in the APD, an internal signal gain, called avalanche multiplication gain (M), is generated through a sub-sequent series of impact ionization (II) events. The multiplication process generates an excess noise factor (F) due to the random position and time of the II-events. The nature of the multiplication process can be described by the effective k-ratio, which is an effective ratio between electron and hole II-rates, with a lower k-ratio resulting in lower excess noise [1]. Furthermore, a low effective k-ratio means a shorter time required to build-up the avalanche gain. This improves the device bandwidth at higher gain. Therefore, a lot of effort is spent in the engineering of better effective k-ratios for APDs. The effective k-ratio depends on the material. Typical multiplication materials for long wavelength telecom and datacom APDs are InP (k ~ 0.5 to 0.6 [2] [3]), In<sub>0.52</sub>Al<sub>0.48</sub>As (k ~ 0.29 to 0.5 [4]) and Silicon (k < 0.1 [5]). The k-ratio also depends on the device geometry. Small structures give rise to non-local impact ionization (e.g. "dead-space" effects [6]). This enabled engineering of lower k-ratio using thin multiplication regions (k ~ 0.15 [7]), engineered hetero-structures (k ~ 0.1 [8]) and superlattice multiplication layers (k ~ 0.25 [9]) which have been demonstrated in high speed III-V APD devices. Recent improvements of the effective k-ratio for III-V APDs include exploring non-conventional material systems (e.g. antimonides

[10], k ~ 0.01 [11]), band-diagram engineering (e.g. staircase multiplication region with extremely low noise [12]) and band-structure engineering through advanced material growth (e.g. digital alloy materials, k ~ 0.15 [13]). These recent advances are certainly promising for low speed, low excess noise APDs. However, the application of these approaches to very high speed APDs (>20 GHz) remains to be demonstrated. In parts, this can be explained through the requirement for short carrier transit times in high speed APDs. Therefore, thin multiplication regions are needed, which require a high electric field to generate sufficient gain. The small dimensions and high electric field are contra-productive for some of these new concepts.

The sensitivity of the receiver improves with multiplication gain and responsivity (R) [14]. At high multiplication gain, the main limitation for the sensitivity for very high-speed telecom and datacom applications is the limited bandwidth provided by the APD [15] and only in second order the APD excess noise and detector dark current. This is due to the strong impact of the high speed TIA on the total receiver noise. The reduction of the APD bandwidth at higher gain causes inter-symbol interference at the desired bit rates at which point the sensitivity decreases. This is slightly different for APDs used in conjunction with low noise amplifiers for sensing applications at a couple of MHz or GHz bandwidth for which sensitivity is limited by the APD excess noise.

The available multiplied-responsivity times bandwidth (M x R x B) product is a first order estimation comparing different technologies with regards to their potential receiver sensitivity at a given bit rate. Fig. 1. reviews M x R x B-products for different examples of high speed APDs found in recent literature [15-19].

Waveguide type APDs offer higher absolute bandwidth at low multiplied responsivity compared to vertical illuminated counterparts. This is mainly due to the possibility to break the

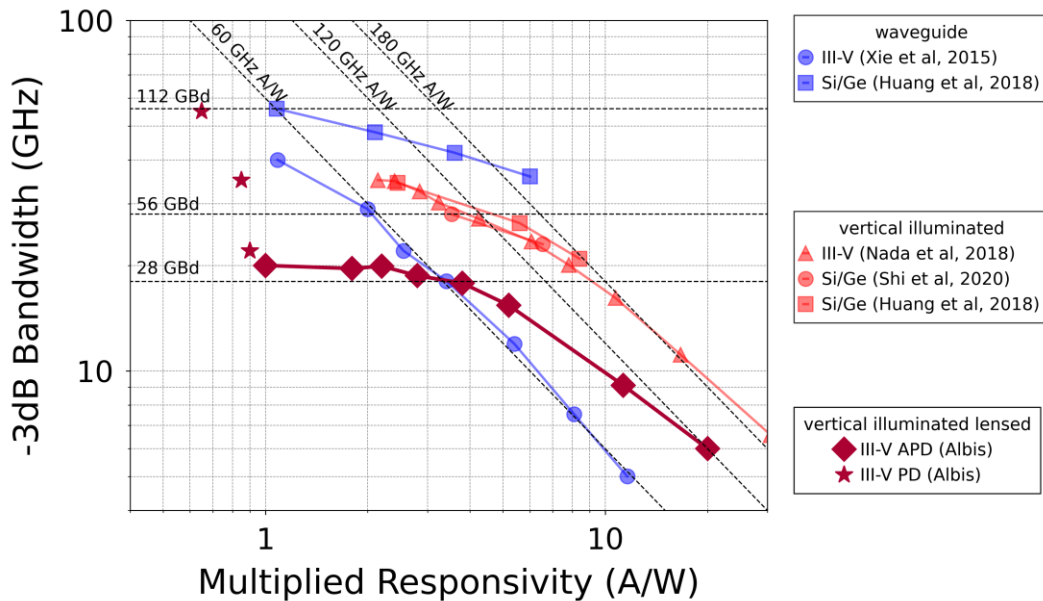


**Fig. 1:** High speed APD from literature in comparison with III-V APD presented in this work. For reference state-of-the-art vertical illuminated III-V PD are shown.

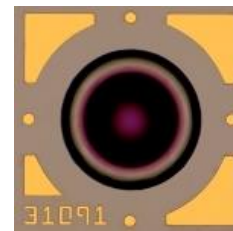
trade-off between transit time and responsivity by separating charge transport in one direction and light propagation in the other. While suited for direct implementation in silicon photonics, a main drawback of stand-alone waveguide APD chips is the coupling efficiency, generally requiring more complex optical setups and introducing polarization dependencies. The side illumination makes the device less convenient to be integrated in standard TO-based receiver optical sub-assembly (ROSA).

For vertical illuminated APDs for 56 GBd, both III-V ( $\text{In}_{0.52}\text{Al}_{0.48}\text{As}$ ) and silicon-germanium (SiGe) based APDs give very similar  $M \times R \times B$  product around 180 GHz A/W. While the gain-bandwidth product of SiGe based APDs is generally better thanks to the low  $k$ -ratio, III-V APDs show better trade-off in terms of transit time and responsivity. At the same time, germanium based APDs show larger dark currents due to lattice mismatch and stress of germanium grown on top of silicon. Therefore, we expect both material systems to provide similar receiver sensitivities in 56 Gbd applications while SiGe has higher potential at higher bandwidth.

The comparison between state-of-the-art vertical illuminated  $\text{In}_{0.53}\text{Ga}_{0.47}\text{As}/\text{InP}$  PIN PDs in Fig. 1 shows the improvement in multiplied responsivity and hence possible sensitivity gains obtainable using APD receiver at different data rates. The current trend indicates that the benefit of an APD in comparison with a PIN PD is becoming smaller for higher data rates which is due to the inherent nature of avalanche build-up time. In order to break this trend new low  $k$ -ratio

concepts ( $k \ll 0.1$ ) with high gain capabilities ( $M \sim 10$ ) and short carrier transit times beyond the current state-of-the-art would be needed.

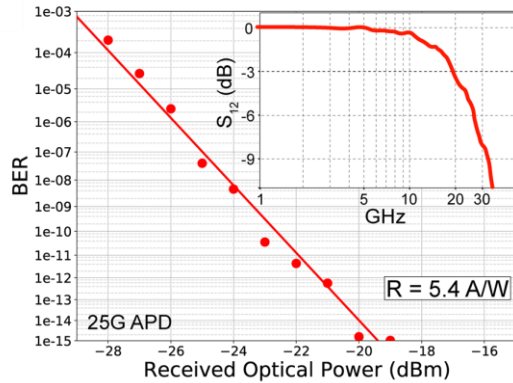
In this talk, we review our III-V APD which is optimized for operation at 10 Gb/s and 25 Gb/s, providing high multiplied responsivity and hence sensitivity (see Fig. 1). A main advantage for this type of APD is the monolithically integrated, backside lens (see Fig. 2) which greatly reduces the coupling losses and hence improves responsivity. It also simplifies the assembly in a TO-can or hybrid integration with waveguides by increasing the alignment tolerances and improving reproducibility of the active alignment process. Furthermore, an emphasis is set on the high dynamic range which is linked to exceptional high optical damage threshold. These requirements are generally neglected in literature but they constitute an important aspect of high speed APD receiver operation.



**Fig. 2:** Microscope picture of monolithically integrated, backside lens. Chip size is 350  $\mu\text{m}$  x 350  $\mu\text{m}$ .

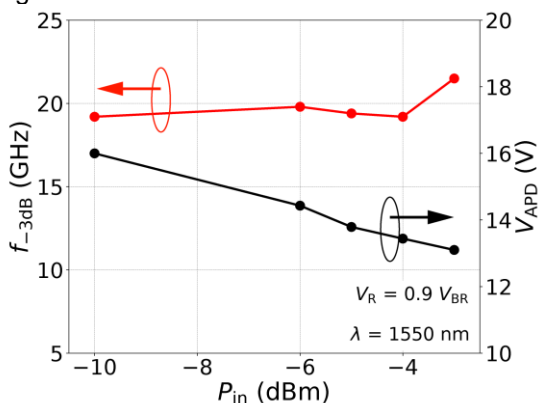
### Sensitivity and dynamic range

Fig. 3 shows the BER for an APD ROSA realized with Albis 25G APD. The multiplied responsivity at operating condition of 90%  $V_{br}$  is 5.4 A/W at wavelength of  $\lambda = 1550$  nm. The measured sensitivity at BER =  $5e-5$  is -27 dBm with ER = 14dB. Similar measurement on 10G APD yield a sensitivity of -34.5 dBm at BER =  $5e-5$  [20].



**Fig. 3:** 25 Gb/s APD receiver measurement. The inset shows the frequency response of the APD chip at 90%  $V_{br}$ .

An additional requirement for high speed telecom and datacom APDs is a high dynamic range from the sensitivity limit up to couple of mW. Since APDs are specifically designed for high sensitivity applications at low optical input power, their application requires a protective series resistance in the biasing path to passively quench the bias voltage and to limit the total device current under high optical power condition. This avoids excessive heat generation and thermal induced damage. Using such series resistor, it is necessary that the APD bandwidth does not collapse up to the overload optical input power which is around -3 dBm. This is demonstrated in Fig 4.



**Fig 4:** -3 dB bandwidth (red) of 25 Gb/s APD as a function of optical input power using a protective series resistance of 8 k $\Omega$  in the biasing path of the APD. Voltage across the APD as function of optical input power (black)

### Optical Damage Threshold

Furthermore, the APD needs to sustain very high

optical input powers in field operation without damage. In the presence of a high optical input power, the passive quenching series resistance causes - as intended - a reduction of the bias voltage across the APD as shown in Fig. 5.

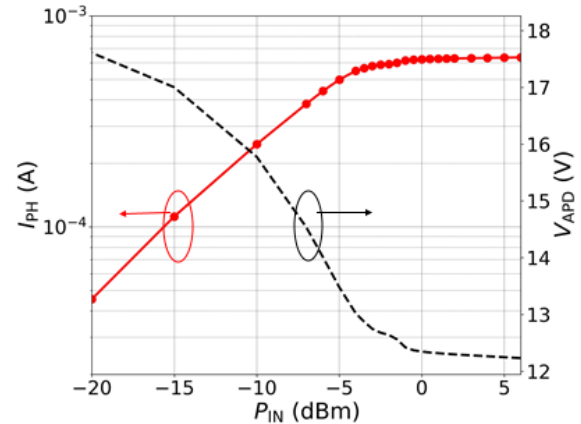


**Fig. 5:** Photocurrent (red) vs. optical input power for 25 Gb/s APD. Voltage across the APD as function of the optical input power (black).

The bias voltage drops until the APD punch-through voltage is reached upon which a condition is established where the photo current, APD voltage, depletion layer reach-through across the hetero-junction and space-charge effect in the absorption layers are balanced. Generic high speed, mesa type separated absorption, charge and multiplication (SACM) APDs may suffer from parasitic device currents under such condition which we call optical saturation induced surface currents (OSICS) [20]. It is paramount to design the mesa APD to avoid these currents which may cause catastrophic failure.

The 25G APD presented in this work shows an optical damage threshold above +6 dBm while the 10G APD remains without damage above +10 dBm using a 8.2 k $\Omega$  series resistance [20]. Finally, the optical damage threshold is screened on a wafer level to guarantee 100% of the devices shipped fulfil the optical damage threshold specifications [21].

### Conclusion

The current state-of-the-art for high speed, long wavelength APDs has been reviewed. We demonstrated high sensitivity, 25 Gb/s APD receivers based on our III-V, vertical illuminated, lensed APDs. The backside integrated lens simplifies the optical alignment process in TO can packages. These APDs offer high dynamic range and exceptionally high optical damage threshold above +6 dBm optical input power which is guaranteed in production by a wafer level testing of each individual APD chip.

## References

- [1] R. J. McIntyre, "Multiplication noise in uniform avalanche diodes," in *IEEE Transactions on Electron Devices*, vol. ED-13, no. 1, pp. 164-168, Jan. 1966, doi: <https://doi.org/10.1109/T-ED.1966.15651>
- [2] Tatsunori Shirai, Susumu Yamasaki, Fukunobu Osaka, Kazuo Nakajima, and Takao Kaneda, "Multiplication noise in planar InP/InGaAsP heterostructure avalanche photodiodes", *Appl. Phys. Lett.* 40, 532-533 (1982), doi: <https://doi.org/10.1063/1.93132>
- [3] J. C. Campbell, S. Chandrasekhar, W. T. Tsang, G. J. Qua and B. C. Johnson, "Multiplication noise of wide-bandwidth InP/InGaAsP/InGaAs avalanche photodiodes," in *Journal of Lightwave Technology*, vol. 7, no. 3, pp. 473-478, March 1989, doi: <https://doi.org/10.1109/50.16883>
- [4] I. Watanabe, T. Torikai, K. Makita, K. Fukushima and T. Uji, "Impact ionization rates in (100) Al<sub>0.48</sub>In<sub>0.52</sub>As," in *IEEE Electron Device Letters*, vol. 11, no. 10, pp. 437-438, Oct. 1990, doi: <https://doi.org/10.1109/55.62988>
- [5] R. Van Overstraeten, H. De Man, "Measurement of the ionization rates in diffused silicon p-n junctions", *Solid-State Electronics*, Volume 13, Issue 5, 1970, Pages 583-608, doi: [https://doi.org/10.1016/0038-1101\(70\)90139-5](https://doi.org/10.1016/0038-1101(70)90139-5)
- [6] M. A. Saleh et al., "Impact-ionization and noise characteristics of thin III-V avalanche photodiodes," in *IEEE Transactions on Electron Devices*, vol. 48, no. 12, pp. 2722-2731, Dec. 2001, doi: <https://doi.org/10.1109/16.974696>
- [7] G. S. Kinsey, J. C. Campbell and A. G. Dentai, "Waveguide avalanche photodiode operating at 1.55  $\mu\text{m}$  with a gain-bandwidth product of 320 GHz," in *IEEE Photonics Technology Letters*, vol. 13, no. 8, pp. 842-844, Aug. 2001, doi: <https://doi.org/10.1109/68.935822>
- [8] Ning Duan et al., "High-speed and low-noise SACM avalanche photodiodes with an impact-ionization-engineered multiplication region," in *IEEE Photonics Technology Letters*, vol. 17, no. 8, pp. 1719-1721, Aug. 2005, doi: <https://doi.org/10.1109/LPT.2005.851903>
- [9] I. Watanabe et al., "High-speed and low-dark-current flip-chip InAlAs/InAlGaAs quaternary well superlattice APDs with 120 GHz gain-bandwidth product," in *IEEE Photonics Technology Letters*, vol. 5, no. 6, pp. 675-677, June 1993, doi: <https://doi.org/10.1109/68.219707>
- [10] Shiyu Xie, Xinxin Zhou, Shiyong Zhang, David J. Thomson, Xia Chen, Graham T. Reed, Jo Shien Ng, and Chee Hing Tan, "InGaAs/AlGaAsSb avalanche photodiode with high gain-bandwidth product," *Opt. Express* 24, 24242-24247 (2016), doi: <https://doi.org/10.1364/OE.24.024242>
- [11] A.H., Jones, S.D., March, S.R., Bank et al., "Low-noise high-temperature AlInAsSb/GaSb avalanche photodiodes for 2- $\mu\text{m}$  applications", *Nat. Photonics* 14, 559-563 (2020), doi: <https://doi.org/10.1038/s41566-020-0637-6>
- [12] S.D., March, A.H., Jones, J.C., Campbell. et al., "Multistep staircase avalanche photodiodes with extremely low noise and deterministic amplification", *Nat. Photonics* 15, 468-474, 2021, doi: <https://doi.org/10.1038/s41566-021-00814-x>
- [13] W., Wang, J., Yao, J., Wang, Z., Deng, Z., Xie, J., Huang, H., Lu, and B., Chen, "Characteristics of thin InAlAs digital alloy avalanche photodiodes," *Opt. Lett.* 46, 3841-3844, 2021, doi: <https://doi.org/10.1364/OL.435025>
- [14] J. Conradi, "A simplified non-Gaussian approach to digital optical receiver design with avalanche photodiodes: theory," in *Journal of Lightwave Technology*, vol. 9, no. 8, pp. 1019-1026, Aug. 1991, doi: <https://doi.org/10.1109/50.84168>
- [15] M. Nada, Y. Yamada and H. Matsuzaki, "Responsivity-Bandwidth Limit of Avalanche Photodiodes: Toward Future Ethernet Systems," in *IEEE Journal of Selected Topics in Quantum Electronics*, vol. 24, no. 2, pp. 1-11, March-April 2018, Art no. 3800811, doi: <https://doi.org/10.1109/JSTQE.2017.2754361>
- [16] S. Xie, S. Zhang and C. H. Tan, "InGaAs/InAlAs Avalanche Photodiode With Low Dark Current for High-Speed Operation," in *IEEE Photonics Technology Letters*, vol. 27, no. 16, pp. 1745-1748, 15 Aug. 2015, doi: <https://doi.org/10.1109/LPT.2015.2439153>
- [17] M., Huang, P., Cai, S., Li, G., Hou, N., Zhang, T., Su, C., Hong, D., Pan, "56GHz Waveguide Ge/Si Avalanche Photodiode", 2018 Optical Fiber Communications Conference and Exposition (OFC), 1-3, 2018, doi: <https://doi.org/10.1364/OFC.2018.W4D.6>
- [18] B., Shi. et al. "106 Gb/s Normal-Incidence Ge/Si Avalanche Photodiode with High Sensitivity", *Optical Fiber Communication Conference (OFC) 2020 M3D.2 (OSA, 2020)*. doi: <https://doi.org/10.1364/OFC.2020.M3D.2>
- [19] M. Huang et al., "Germanium on Silicon Avalanche Photodiode," in *IEEE Journal of Selected Topics in Quantum Electronics*, vol. 24, no. 2, pp. 1-11, March-April 2018, Art no. 3800911, doi: <https://doi.org/10.1109/JSTQE.2017.2749958>
- [20] A., Ciarrocchi, W. Quan, M., Hämmerli, H. Meier, "Long-Wavelength Avalanche Photodiodes Operating over a 30dB Optical Input Power Range", *ECOC 2022*, publication pending.
- [21] A. Ciarrocchi, W. Quan, M. Blaser, M. Hämmerli, and H. Meier, "Optical Damage Threshold Screening Methodology for 28 GBd, Long Wavelength Avalanche Photodiodes," in *Optical Fiber Communication Conference (OFC) 2022*, doi: <https://doi.org/10.1364/OFC.2022.Th2A.39>